DOI: 10.13009/EUCASS2023-801
Aerospace Europe Conference 2023 – 10TH EUCASS – 9TH CEAS

Hydrogen generation from aluminum composites hydrolysis for space propulsion

Alberto Verga [(1)], Michela Ferri [(1)], Alberto Verga [(1)], Barbara Vercelli [(2)], Riccardo Donnini [(2)], Stefano Dossi [(3)], Alessandro Murgia [(3)], Giovanni Gianola [(3)], Luciano Galfetti [(1,3) †]

[(1)] Politecnico di Milano
Space Propulsion Laboratory
Aerospace Science and Technology Department
Via La Masa, 34 I-20156 Milano, Italy

alberto.verga@mail.polimi.it
michela.ferri@mail.polimi.it
alberto.verga@polimi.it
luciano.galfetti@polimi.it

[(2)] CNR-ICMATE, National Research Council of Italy
Via Roberto Cozzi 53, I-20126 Milano, Italy

barbara.vercelli@cnr.it
riccardo.donnini@cnr.it

[(3)] ReActive - Powder Technology
Via Lambro 7, I-20068 Peschiera Borromeo, Milano, Italy

stefano.dossi@reactivepowders.com
alessandro.murgia@reactivepowders.com
giovanni.gianola@reactivepowders.com

† Corresponding author: Luciano Galfetti, Via La Masa, 34 I-20156 Milano, Italy e-mail: luciano.galfetti@polimi.it

Abstract

Hydrogen is a green energy source, largely used in space propulsion. Drawbacks are transport and storage due to safety and volumetric reasons. These problems can be solved by aluminum hydrolysis. Aluminum exothermically reacts with water to produce hydrogen and non-toxic Al hydroxides and oxides. The oxide layer around the metal particles, inhibiting the reaction, can be removed by chemical or physical activation processes. Once aluminum is activated, the Al-water reaction satisfies the requisite of an in-situ and on demand hydrogen generation, overcoming the storage and handling issues. The activation of aluminum powders, its effects on the Al-water reactions, supported by SEM and XRD analyses, are discussed. Hydrolysis of ball-milled aluminum composites is used for a proof of concept of a water propulsion system, with on-board hydrogen generation.

1. Aluminum hydrolysis

Hydrogen is the most abundant observable element in the universe. Colorless, odorless, tasteless and highly flammable, with a boiling point of 20.27 K and a melting point of 14.02 K, in bound state is present in water (11.19 %) and forms compounds with most elements. It is the main constituent of stars, while on Earth it is scarcely present in the free, molecular state. As a consequence it must therefore be produced. Hydrogen can be obtained from different sources, such as fossil fuels, biomass, and water. As for the first option, the most economical way to obtain hydrogen is the steam reforming of methane, which has, though, the serious drawback of greenhouse emissions, considering that approximately 2.5 tonnes of carbon are released (as CO_2) for each tonne of hydrogen produced. A second way of hydrogen generation is water electrolysis, which however requires large amounts of power and has a low energy efficiency. A third way is to release hydrogen via the hydrolysis with water, which gives the opportunity to make hydrogen generation on-demand, on-site, in real-time. Aluminum has been identified as one of the best substances for the on-site hydrogen generation, avoiding hydrogen storage and transport. It is an energy carrier that can deliver significant amount of energy, with a high calorific value and clean combustion. The need to generate green hydrogen

DOI: 10.13009/EUCASS2023-801

is driving the search for alternatives such as biomass composition, photolytic water decomposition and hydrolysis of metals and metal hydrides [10]. In particular, metal hydrolysis is an appealing option and has several advantages. Water is easily accessible, metal powders are safely storable, transportable and have a long shelf life if protected from moisture. Furthermore, besides hydrogen and thermal energy, the only byproducts of metal-water reactions are metal oxides or hydroxides, that in most cases are chemically inert, easy to collect, and suitable to be reprocessed back to pure metals.

A preliminary study on the maximum theoretical yield of the reaction is obtained by the stoichiometry and displayed in Figure 1.1 (A), together with the reaction heat (B). High specific energy metals, as aluminum, boron, magnesium and silicon have the highest gravimetric yield while a greater hydrogen yield per unit volume is observed for high density metals, as manganese, chromium or again aluminum. Concerning the completeness, which is an index of the reaction efficiency, the most attractive powders are magnesium, manganese, aluminum and chromium.

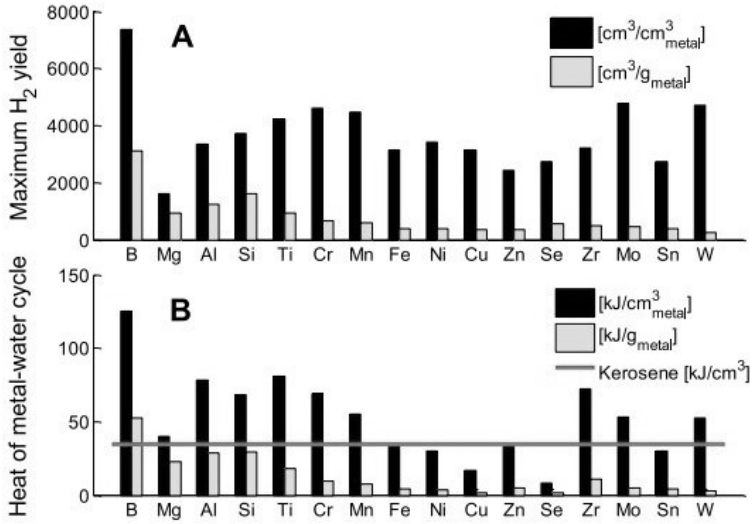

Figure 1.1. A: Volumetric and gravimetric maximum hydrogen yield
B: volumetric and gravimetric reaction heat of the metal-water cycle [1].

Among the metals just mentioned, aluminum has the highest hydrogen yield per gram and a yield per volume lower only to the one of manganese but, differently from Mn, it has a significant production also at low temperatures. It has also a significant efficiency, comparable to magnesium and manganese. Moreover, aluminum is abundant and cheap and its costs can be further reduced if powders are obtained from waste aluminum products. Aluminum is therefore the selected metal for the investigation in this study.

Depending on the amount of water reacting with aluminum, three possible reactions can occur:

$$2\,Al + 6H_2O \rightarrow 2Al(OH)_3 + 3H_2 \quad \Delta H_{r,298} = -839\ kJ/mol \tag{1.1}$$

$$2\,Al + 4H_2O \rightarrow 2AlO(OH) + 3H_2 \quad \Delta H_{r,298} = -862\ kJ/mol \tag{1.2}$$

$$2\,Al + 3H_2O \rightarrow Al_2O_3 + 3H_2 \quad \Delta H_{r,298} = -950\ kJ/mol \tag{1.3}$$

The reactions have the same stoichiometric coefficients for Al and H_2 meaning that from 1 g of aluminum 1.36 L of hydrogen are obtainable (at standard condition, 1 atm and 25 °C). All the reactions are highly exothermic. The most stable product in the range of temperature from 20 to 280 °C is $Al(OH)_3$, from 280 to 480 °C is AlO(OH), while above 480 °C is Al_2O_3 [22]. Although the aluminum-water reaction is spontaneous, aluminum reacts with the oxygen in the air to create a protective layer of aluminum oxide Al_2O_3, also called alumina, which hinders the spontaneity of the reaction. For this reason, efficient methods to catalyze the reaction or remove the alumina layer need to be investigated to boost the H_2 production.

Al powders increase the surface area of the reaction and consequently hydrogen generation. An increase in water temperature enhances the diffusion of the oxidizing species and the hydration of the Al_2O_3 shell, reducing the induction time [1] – [2]. High pH solutions react with the alumina layer bringing to its disruption and the high concentration of OH seems to catalyze the Al corrosion. Acid solutions, also, improve the oxide erosion, but the overall catalytic effect on the reaction has been less studied compared to alkaline solutions [3] – [4]. The presence of more noble alloying metals, such as Bi, Fe or Ni, catalyzes the galvanic reaction of aluminum with water and induces the phenomenon of

DOI: 10.13009/EUCASS2023-801

pitting corrosion. The drawback is the reduction in the mass fraction of aluminum implying a reduction in the total hydrogen produced. Metal additives as Li and Mg, can directly produce hydrogen reacting with water, thus enhancing the overall hydrogen production and yield. Non-metallic additives have shown the capability to enhance Al hydrolysis. For example, graphite favors the galvanic corrosion and induces defects that increase the reaction surface, organic fluoride boosts the reaction yield and rate while metal hydrides (LiH, CaH_2...) improve the total hydrogen generation and its performance [3].

Probably, the best way to improve aluminum hydrolysis reaction is the mechanical activation. Al can be activated to react with water in standard conditions by mechanical treatments that disrupt the protective Al_2O_3 layer. The most common technique is ball milling, in which aluminum powders are impacted and squeezed by milling balls during high-speed operation. The process causes defects, dislocations and cracks in the aluminum particles, thereby increasing their specific surface area and damaging the original dense alumina film. Due to the good ductility of aluminum, particles also tend to wield during the milling and this phenomenon can be exploited to dope them with additives that adhere to the surface and enter their interior. The resulting particles from ball milling all exhibit a damaged Al_2O_3 layer and irregular and grooved structures that strongly increase the surface of reaction [3]. The addition of salts to the Al powders previous the mechanical activation promotes the process. During milling, salts, due to their brittle nature, are crushed in fine particles that adhere to the Al surface and prevent excessive cold wielding that would lead an increase of dimension of the powder. During the reaction, the salts dissolve into water leading to the exposure of fresh Al, thus fastening the hydration process. Finally, the ions resulting from the salt dissolution tend to promote the charge transfer in the micro galvanic cells of the composite Al powders [5].

Concerning reaction byproducts, all the possible byproducts of the reaction are non toxic. Possible byproducts of the Al-water reactions are $Al(OH)_3$ and AlO(OH). In addition to this, also the heat released by the process is correlated to byproducts, with a slightly lower enthalpy of reaction in case of $Al(OH)_3$. The study of the hydrolizates is therefore fundamental to fully exploit the reaction for energy purposes as the hydrogen and the heat generation. Considering portable and vehicular application of the Al technology for hydrogen production, the volumetric efficiency becomes extremely important. The drawback from this point of view is represented by the lower density of water (~ 1000 kg/m^3) compared to aluminum (2700 kg/m^3). Also, the investigation of the byproducts is relevant as the water consumption of the reaction that brings to AlOOH is 33% less than the one that leads to $Al(OH)_3$ as can be seen from the stoichiometry in Eqs. (1.1) and (1.2) [6] – [7].

All the reactions of aluminum with water (Eqs. (1.1) - (1.3)) are strongly exothermic. Considering 1 kg of aluminum, 0.11 kg of hydrogen could be theoretically produced with a heat release ranging from 4.2 kWh to 4.3 kWh at 25 °C. Taking into account the higher heating value of the produced hydrogen, the total specific energy of Al amounts to 8.7 kWh/kg, or 23.5 MWh/m^3 of solid Al at 25 °C. Thus, the volumetric energy density of Al is more than two times higher than the ones of mineral oils. This property makes aluminum a highly interesting candidate as energy carrier [8] - [9]. A summary is reported in Fig. 1.2, from [8].

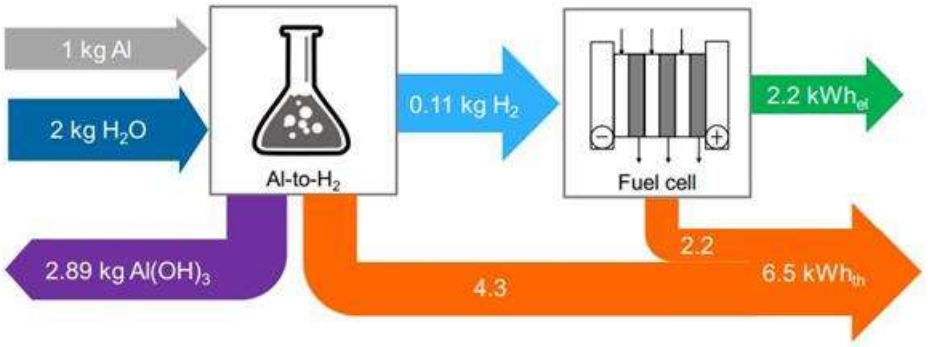

Figure 1.2: Heat and electricity production from the oxidation of aluminium with water, assuming a fuel cell electric efficiency of 50% [8].

2. Production and characterization of activated aluminum powder

The thin, coherent, adhering layer of aluminum oxide on the aluminum surface strongly hinders the reactivity with water, also for powders. For this reason different techniques are used to activate aluminum powders. This section discusses the activation of aluminum composite powders, which are then analyzed by laser diffractometry, XRD, SEM and EDS to investigate the powder morphology and identify their various phases.

DOI: 10.13009/EUCASS2023-801

2.1. Powder Production

The starting materials in order to obtain aluminum composites are Al powder (mean size, D[4,3] = 46 μm), Bi powder (D[4,3] < 44 μm, 99.5% purity) and NaCl (99.5% purity). Bismuth is a galvanic catalyst thanks to its good hydrolysis performances shown by Al-Bi composites. Bi content higher than 10% proved to have a hydrogen conversion efficiency of 100 % at room temperature [10]. NaCl is an easily available and low cost salt promoter, which makes it a suitable candidate for future applications of the technology.

The effect on hydrogen production of different percentages of additives in the powder is investigated in [11]. The composition 90% Al - 5% Bi - 5% NaCl resulted to be the one with the highest performances in terms of yield and total hydrogen production per gram of powder. This composition is considered the most adequate to test the effects of temperature and pressure on hydrogen production and rate, due to the large content of aluminum available to react with water. Another composition, consisting of 80% Al - 10% Bi - 10% NaCl, is investigated but, due to the elevated amount of additives, its usage in the tests at various pressure and temperature has been disregarded. Indeed, preliminary experiments showed an extremely high reactivity, likely to overshadow the effect of the thermodynamic conditions on the reaction. In addition, the reduced quantity of aluminum makes this composition less attractive in the field of hydrogen production. However it is effectively used for propulsive purposes because of its enhanced reactivity.

The composite Al-Bi-NaCl powders are prepared by ball milling using a Retsch PM100 planetary ball miller. Settings for the milling in terms of time and speed are analysed in [12]. The milling speed is in the range 200-500 rpm and the activation time between 40 min and 12 h, but high speed of rotation (500 rpm) have been tested only up to 2 h. These conditions lead to unsatisfying results in terms of hydrogen generation. The behaviour of the powder with milling time in the range 1-6 hours at 500 rpm is studied by [13]. The yield increases with the milling time until 4 hours are reached. Extending the duration up to 6 hours does not show a significant increase in the yield. Considering these results, in this work the effective milling time is set to 4.5 hours, corresponding to 6 hours of miller operational time, accounting for the activation/pause time introduced to inverse the rotation and to avoid overheating. The ball milling parameters are listed in Table 2.1. The tuning of the settings has been done employing a 90% Al - 5% Bi - 5% NaCl powder composite since its mechanical activation conditions are more stringent due to the reduced amount of catalysts.

2.2. Powder characterization

The size of the particles is investigated by laser diffractometry using Malvern Scirocco 2000 particle size analyzer. The starting aluminum pure powder, the 80% Al - 10% Bi - 10% NaCl composite, and the 90% Al - 5% Bi - 5% NaCl are both analyzed. Scanning Electron Microscopic (SEM) analyses are carried out to investigate the micromorphology of the pure powders and of the 90% Al - 5% Bi - 5% composite. X-ray diffraction (XRD) spectra are recorded using a Siemens D500 X-ray diffractometer with Cu-Kα radiation (λ = 0.15418 nm) and collected in the 2θ range of 10°- 80°, with a step size of 0.1° and 5 s/step. These analyses are carried out on the 90% Al - 5% Bi - 5% NaCl composites. Finally, Energy Dispersive X-ray Spectroscopy (EDS) analyses are performed to map the element content in the 90% Al - 5% Bi - 5% composite powders. The SEM and the EDS analysis are carried out using the SEM-FEG SU70 Hitachi microscope.

Table 2.1: Ball milling parameters.

Parameter	Value
Composition	90% Al–5% Bi–5% NaCl
Milling balls material	Steel AISI 440-C
Milling balls size	10 mm and 8 mm
BPR	20:1
Ball milling speed	550 rpm
Ball milling time	6 hr
Activation / pause time	45 s / 15 s
Ball milling atmosphere	Helium

Table 2.2: Malvern analysis results for the investigated powders.

Composition	SSA m^2/g	D[3,2] μm	D[4,3] μm
Pure Al	0.23	26	46
90% Al-5% Bi-5% NaCl	0.03	197	342
80% Al-10% Bi-10% NaCl	0.32	19	33

2.2.1. Particles size

The Malvern Panalytical measures the particle size distribution and important parameters as the specific surface area of the powder (SSA), the De Brouckere volume-weighted mean diameter D[4,3] and the Sauter surface-weighted mean D[3,2]. Results are shown in Table 2.2. Since a powder presents particles of different shape and dimensions, its

DOI: 10.13009/EUCASS2023-801

characteristics are resumed in one parameter referring to equivalent spheres, of the same diameter, that retains some property of the original powder.

Table 2.3: Malvern analysis results for the investigated powders.

Composition	SSA m^2/g	D[3,2] μm	D[4,3] μm
Pure Al	0.23	26	46
90% Al - 5% Bi - 5% NaCl	0.03	197	342
80% Al - 10% Bi - 10% NaCl	0.32	19	33

The results, reported in Table 2.3, show that the milling procedure with the 90% Al - 5% Bi - 5% NaCl composite is characterized by cold welding. The D[4,3] increases from the 44 μm of the initial aluminum powder to 342 μm. The D[3,2] is slightly decreased, probably due to a change in the shape of the particles. Considering the 80% Al - 10% Bi - 10% NaCl composite, instead, the milling induces a reduction of the size of the particles compared to the original powder. The higher content of salt prevents the welding and favors the grinding process, as expected. The SSA of this composition is higher of one order of magnitude with respect to the other one, explaining the enhanced reactivity that makes this powder suitable for propulsive applications.

2.2.2. SEM results

Figures 2.1-2.2 show the micro-morphology of the composite powder before and after ball milling. The original Al powder presents a poly-dispersed morphology consisting of large spherical aggregates with dimensions around 40 μm (Figure 2.1a), in agreement with the Malvern analysis, surrounded by smaller spherical particles ranging from 11 μm to 1.5 μm (Figure 2.1b). Bi powders as a whole look smaller than Al ones (Figure 3.1c). They are composed of large spherical aggregates of about 45 μm (Figure 2.1c), comparable to the ones of Al powders, surrounded by spherical particles smaller than Al ones, with diameters ranging from 3 μm to 0.3 μm (Figure 2.1d and Figure 2.1d'). After ball milling, the composite consists of flat blocks with variable dimensions around 500 μm (Figure 2.2e and Figure 2.2e'), which are larger than the original Al and Bi particles. The bigger dimensions compared to the D[4,3] are due to the flattened shape. The blocks show a thick lamellar morphology which is the result of the layered packing/agglomeration of thinner lamellas (see section photograph in Figure 2.2f). These results are consistent with literature reported data [14], according to which the agglomeration of the composite into large blocks is due to the cold-welding between the Al powders, during the first stages of the milling process. In particular, Figure 2.2f shows also the presence of internal microscopic defects that are supposed to favor the hydrolysis process [14].

2.2.3. XRD results

Figure 2.3 shows the XRD patterns of the 90% Al - 5% Bi - 5% NaCl composite powder and tablet. Tablets of compressed powder are investigated for a suitable handling and storage of the activated powder in space propulsion applications. This specific issue is not dealt with in this paper, except for this interesting comparison of the XRD patterns, briefly discussed below. The typical diffraction peaks of Al, Bi, and NaCl can be identified in the powder sample. In particular, the peaks at $2\theta = 77.89°$, 65.02°, 44.70°, and 38.26° correspond to (311), (220), (200) and (111) of Al, at $2\theta = 70.73°$, 62.43°, 56.00°, 48.53°, 39.61° and 26.95° correspond to (214), (116), (024), (202), (104) and (012) of Bi and $2\theta = 31.70°$ correspond to (200) of NaCl [10] – [14]. The XRD spectra suggest that the ball-milling treatment does not affect the phase composition of the composite. No diffraction peaks due to metal oxides and/or hydroxides are present. The behavior of the composite tablet shows also the presence of Al_2O_3 (corundum) and Bi_2O_3 (possible $Bi(OH)_3$). In particular, the peaks at $2\theta = 42.56°$ and 36.05° correspond to (113) and (110) of Al_2O_3 (corundum), and $2\theta = 28.58°$, 30.07° and 32.01° correspond to (201), (220) and (220) of Bi_2O_3 [14] - [15].

DOI: 10.13009/EUCASS2023-801

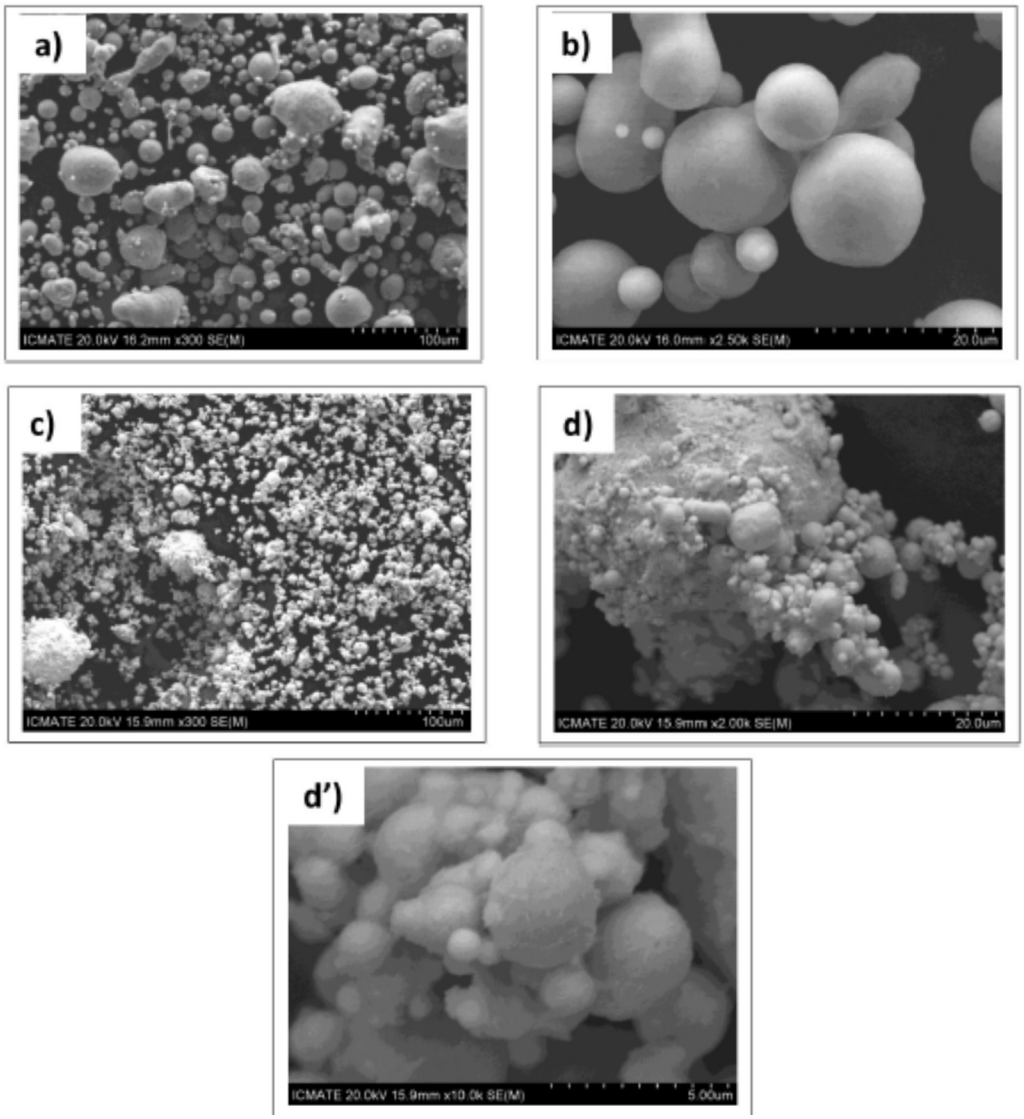

Figure 2.1: SEM images of
Al powders: a) and b)
and Bi powders: c), d) and d').

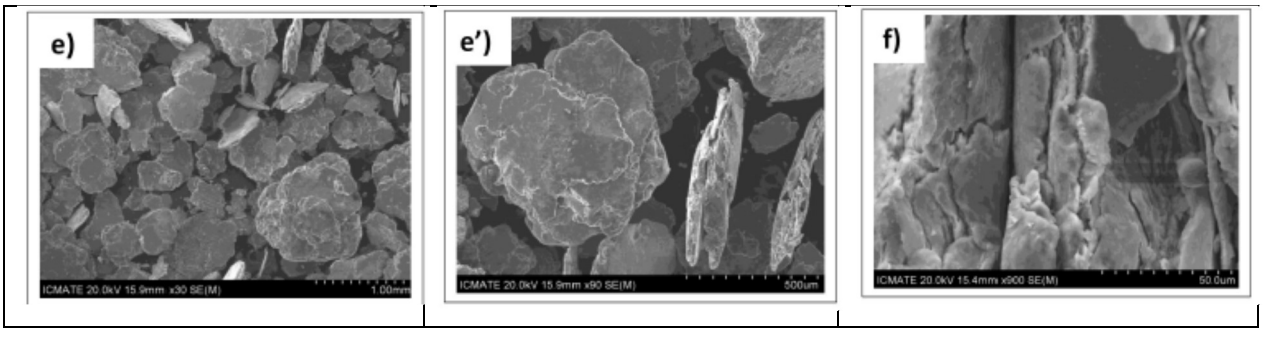

Figure 2.2: SEM images of
Al/Bi/NaCl composite powders: e), e') and f).

It seems that the pressing procedure at 200 MPa brings to the formation of some oxides. This is likely due to the heat generated by the friction of the pin inside the mould. The analysis of pressed powder allows to observe the crystal

DOI: 10.13009/EUCASS2023-801

structure of oxides, which is not evident in free powder. The oxidation of a small quantity of Al causes the reduction in hydrogen conversion efficiency (1 - 2 %) of tablets compared to free powder, observed by Bramani in his MSc dissertation [11].

2.2.4. EDS results

EDS mapping and the results of elemental content (Figure 2.4a) show that Bi, in the composite, is distributed on the surface of the Al matrix. The investigation depth of EDS is around 3 μm, so the white area of the spectrum surface, which shows no elements, can be inferred to have pits deeper than 3 μm. Furthermore, from the SEM backscattered images (Fig 2.4b) it is possible to note that Bi is uniformly attached to the Al matrix without agglomeration in large aggregates (it is verified that the white spots present in the backscattered image are not due to the presence of Bi). The uniform distribution of Bi means that there are more reactive sites that enable a sequence of localized galvanic reactions promoting and sustaining the whole hydrolysis process [16]. Noteworthy, the difference between the mass fraction Al:Bi in the composite (20.49:1; 82.39:4.02) and the one in the starting material (18:1; 5.4:0.3) is in the range of the EDS analysis experimental error. Thus, it may be supposed that the stainless steel balls and jar do not release material in form of powder to the composite during the milling process.

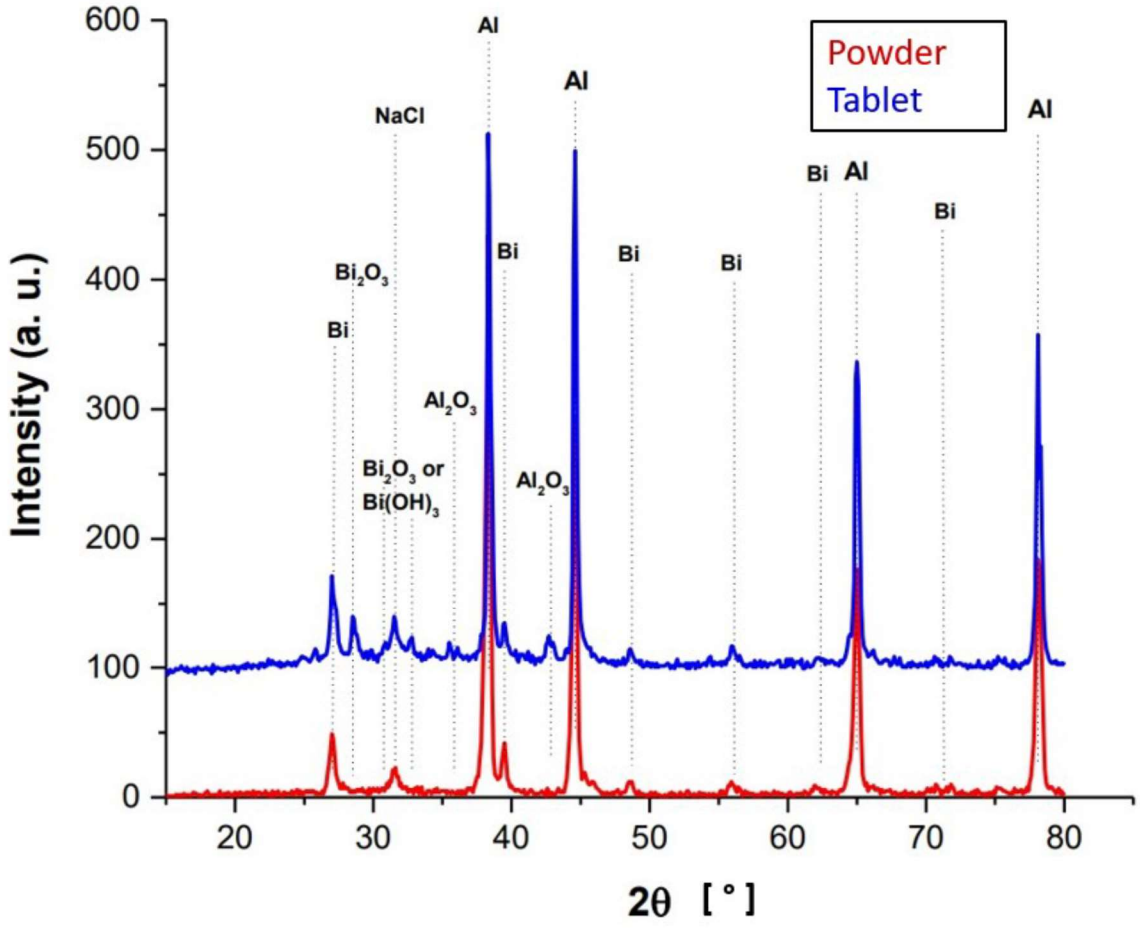

Figure 2.3: XRD patterns of 90% Al - 5% Bi - 5% NaCl composite powder and tablet.

DOI: 10.13009/EUCASS2023-801

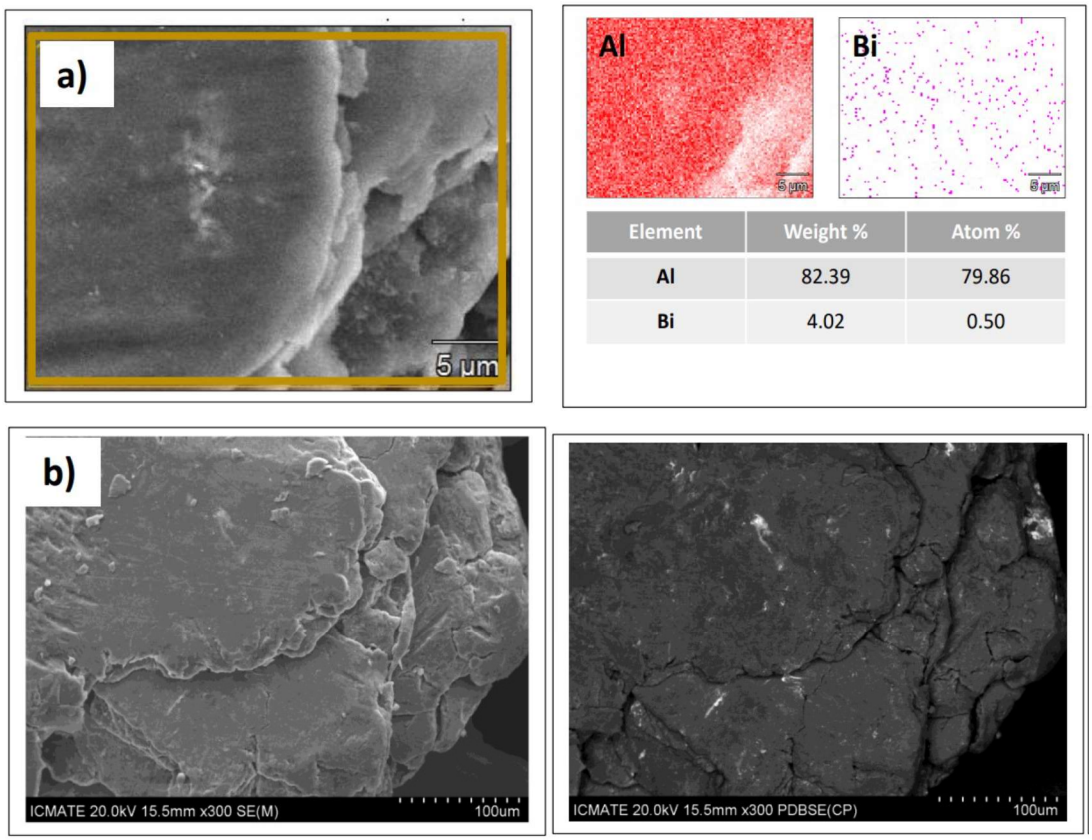

Figure 2.4: 90% Al - 5% Bi - 5% NaCl composite powders
a) EDS mapping.
b) SEM and back-scattered images.

3. Hydrogen production

In order to assess the effects of temperature and pressure over the aluminum-water reaction, a batch reactor has been designed and manufactured. The essential properties of this system are to prevent mixing of the produced hydrogen with air, to allow the analysis of the reaction products, and to measure the reaction rate.

The experimental setup, displayed in Figure 3.1, consists of two main chambers: a pressurizing vessel and a reactor. The pressurizing vessel stores and pressurizes the water that reacts with the aluminum powder. The chamber is connected through a pressure regulator (0-8 bar) to the compressed air piping system. The tank pressure is regulated by an Arduino Uno board that opens a solenoid-valve each time the pressure read by a pressure transducer exceeds the one required for the experiment, defined using a potentiometer. The upper cap of the reservoir internally mounts a support containing a Time of Flight (TOF) distance sensor that measures the level of water inside the container. The sensor, as the electro-valve and the transducer, is connected to the microcontroller. The board directly communicates the values of pressure and water level to a PC, using USB serial communication. PUTTY, a free and open-source serial console and network file transfer application, is used to monitor the status of the test and to save the log in a .txt file.
The reactor is connected at the bottom to the hydraulic pipe coming from the water tank. A manometer measures the reaction pressure. The reactor top cap has three passing holes. Two of them are for the passage of two thermocouples, the first one for the measurement of temperature inside the reactor, the second for the temperature of the water inside the box containing the aluminum powder. The data from the thermocouples are logged to the PC by USB communication using PicoLog data acquisition system. The last opening in the reactor top cap allows the mounting of a faucet (V4). At the beginning of the experiment it is opened to expel the air from the chamber and as soon as the reactor water filling is completed, it is closed to guarantee a constant pressure for the reaction. The water is treated as incompressible; at the end of the procedure, it is opened to discharge the hydrogen produced from the water hydrolysis. The reactor temperature and, as a consequence, the water solution temperature is regulated by a tape resistor wrapped around its main body. The hydrogen is slowly discharged into an inverted graduated column full of water to measure the hydrogen amount produced in the test. Hydrogen can also be discharged into tanks to perform further analysis.

DOI: 10.13009/EUCASS2023-801

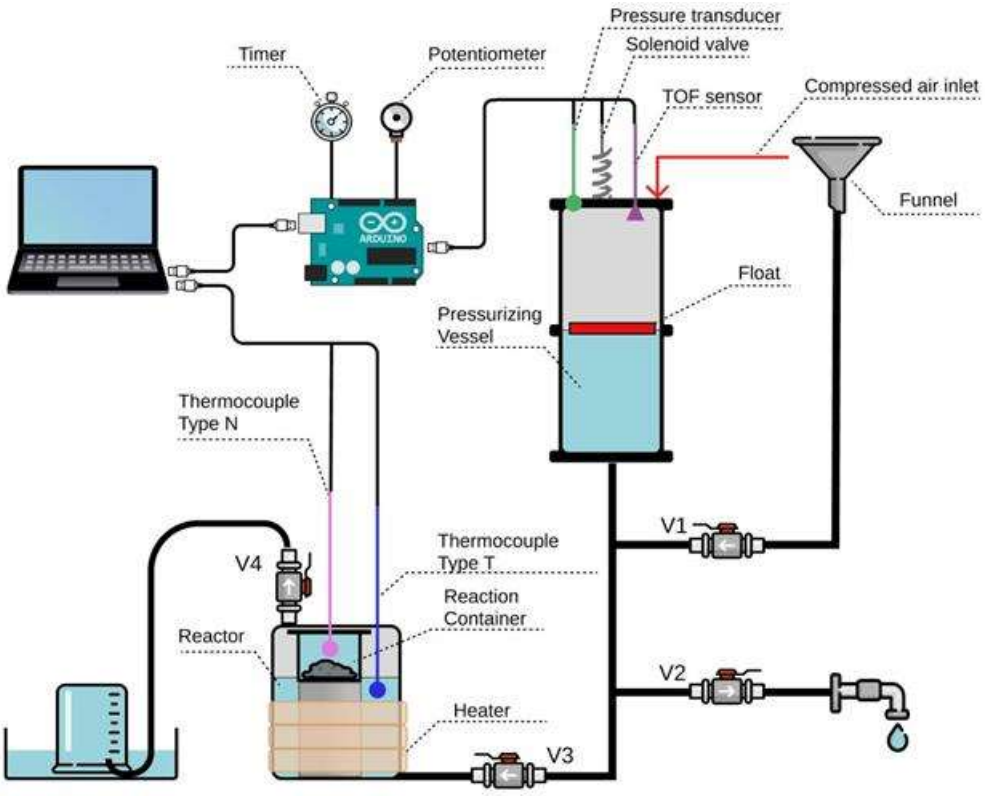

Figure 3.1: Experimental setup layout.

For the whole system:

$$\nabla p + \rho g z = 0 \tag{4.1}$$

In the reactor, the hydrogen produced by the reaction occupies a volume that causes an increase of the water level in the other chamber (the pressurizing vessel), since pressure is kept around the required value by the vent of the electro-valve. From the measurement of the level in the pressurizing tank, knowing temperature and pressure, the mass of hydrogen produced in time is estimated using the equation of state of perfect gas Eq. (4.2):

$$mH_2 = pVMm_{H2} / RT \tag{4.2}$$

in which the hydrogen volume V is equal to the variation of volume in the water tank given by:

$$V = (d_i - d)A_t \tag{4.3}$$

where d_i is the initial level of water, d the one measured instantaneously, and A_t the area of the pressurizing vessel. The pressurizing vessel and reactor geometrical properties are reported in Table 3.1.

Table 3.1. Pressurizing vessel and reactor geometrical properties.

Pressurizing vessel		Reactor	
Internal diameter	83 mm	Internal diameter	101.5 mm
Height	460 mm	Height	179 mm
Thickness	2 mm	Thickness	12.5 mm
Area	5411 mm^2	Area	8075 mm^2
Internal volume	2.49 L	Internal volume	1.45 L

Concerning the pressurizing vessel, the top cap design involves four threaded passing holes, respectively for the pressure transducer (acquisition frequency 50 Hz, full scale 5 bar), the electro-valve (Peter Paul Electronics, series 20 model H22), the connections to the TOF distance sensor (VL53L0X, which emits 940 nm infrared light with a cone angle of 27°), and the compressed air inlet. VL53L0X is chosen for its sensitivity, its reduced field of view and its

DOI: 10.13009/EUCASS2023-801

compatibility to Arduino. 1 mm sensitivity allows to characterize a variation of the water level even when the total displacement is around 2 cm, as expected in the experiment at 4 bar with 0.5 grams of Al powder. A PETG disk float with a Teflon cover is placed in the tank to further increase the precision of the sensor that has to impinge on a surface with high reflectivity [17]. The bottom cap connects the chamber with the system through an hydraulic pipe.

The aluminum-water reaction is confined in a small container placed inside the reactor at the top of the cylindrical steel body. The purpose of the container is to avoid the dispersion of the powder and of the products inside the reactor, simplifying cleaning operations and collection of the byproducts slurry. The container is a 3D printed PETG cylindrical body closed by an interlocking cap. A N type thermocouple measures the temperature inside the container to trace the development of the exothermic reaction. A T type thermocouple measures the temperature at the top of the reactor chamber. This is the value used in Eq. (4.2) to estimate the mass of hydrogen produced. In the initial phases of the test, the temperature is that of the water inside the reactor, but as approximation it is assumed equal to the one of the produced hydrogen. An error analysis validates this assumption since the overall uncertainty is not so sensitive to the temperature. A silicon rubber heat tape is winded up around the reactor. The resistance, regulated through a knob, can reach the maximum temperature of 218 °C. An Arduino Uno controls the pressure of the system and supervises the water levels inside the water tank. The board is connected to a potentiometer, a digital switch, the pressure transducer, the TOF sensor and the electro-valve. The switch starts the timer of the test, while the potentiometer allows the operator to change the relief pressure of the electro-valve.

Effects of water temperature and pressure over aluminium hydrolysis are investigated for the 90 wt% Al - 5 wt% Bi - 5 wt% NaCl composite powder, mechanically activated by ball milling, described in Section 2.1. Results are shown in Figure 3.2.

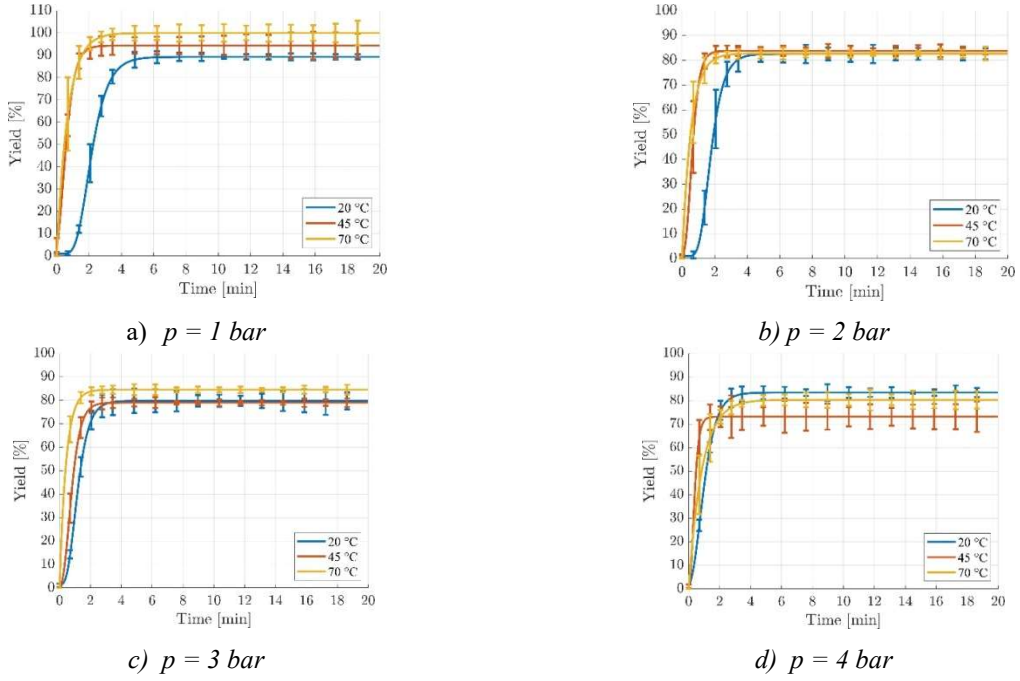

a) *p = 1 bar* b) *p = 2 bar*

c) *p = 3 bar* d) *p = 4 bar*

Figure 3.2: Effects of temperature, in the range 20 – 70 °C, measured at different pressures.

Hydrogen yield and reaction rate vs pressure, in the range 1 – 4 bar, and temperature, in the range 20 – 70 °C are investigated. For each combination, the test is repeated three times. High temperatures decrease the induction time and increase hydrogen growth rate. The only exception is at ambient pressure condition (Figure 3.2a), where higher temperatures favor the total produced hydrogen. This occurs because the high temperature and relatively low pressure cause the build-up of small quantities of vapor that is read as hydrogen by the apparatus. Despite this, the results are consistent with the observations made by [10], in which highly activated Al-Bi-NaCl composites show little or no dependence of the final yield on the starting reaction temperature. This suggests that an effective mechanical activation leads to good hydrogen conversion regardless of the water temperature. It is important to underline again that the temperature indicated refers to the one at the beginning of the test. The reaction container confines the process in a reduced volume in which the powder reacts with approximately 30 mL of water. The container is initially able to exchange water with the reactor but, as soon as the hydrogen is produced, the mixing is shut off by the column of

DOI: 10.13009/EUCASS2023-801

hydrogen. The water level in the reactor moves below the box and only the water trapped inside can react. These conditions lead to a non-isothermal system, in which the water is heated by the exothermicity of the reaction.

4. Water propulsion for micro-propulsion systems

Since 2010 both the launch of micro- or nano-satellites and the research on micro-propulsion have expanded. CubeSats, with their low mass, small volume and power constraints have strong limitations on the resources that can be allocated to the propulsion system. Both chemical and electric propulsion have been proposed for CubeSat applications, but the limited on-board power restricts the use of highly fuel-efficient electric systems, whereas the chemical ones have scaling related issues. Moreover, there are some common problems such as low thrust performance or higher dry mass fraction because of high-pressure gas systems such as tanks, feed lines and valves. Nevertheless, in the near future, CubeSats will require to be equipped with a propulsion unit, especially when involved in formation flights or constellations. Water can be stored in liquid phase, allowing the design of propulsion systems at low pressure with a consequent reduction of dry mass ratio and simplification of feed line routing by using soft tubes. In addition, water is as an ultra-green propellant because of its storability, non-flammability and non-toxicity [18]. For CubeSats, miniaturization of every subsystem is mandatory, and especially the propulsion subsystem is involved in such a reduction in weight and size. Propulsion capability is needed onboard for the adjustment of the trajectory, according to the mission objective, as well as for attitude control. In order to meet these propulsion needs, small sized, low-thrust, small impulse bit (I-bit) systems are required. For Cubesats, suitable propulsion hardware does not exist and new advanced micro-propulsion technologies need to be developed.

The possibility to generate hydrogen on-board releasing at the same time a significant amount of heat makes the Al-water reaction a good opportunity to conceive an innovative micro-propulsion system. The main advantages are safety, a low-pressure gas system allowing to save weight and volume, and a short-span development. Currently, the most promising systems respecting these requirements use water as propellant.

Some of the most relevant technologies are here reported. AQUARIUS is a micro-resistojet propulsion system developed by the University of Tokyo since 2016. The propulsion unit is quite simple, consisting of a tank, a vaporization chamber, pre-heaters and nozzles. A schematic layout [18] is shown in Figure 4.1. Water, stored in a bladder inserted in the tank, is first vaporized at saturated vapor pressure (< 5 kPa) and at room temperature (290-310 K). Then the saturated vapor flows under its own pressure to the thrusters, which are pre-heated to 343 K. Finally, the steam is expelled from the thrusters [18] - [19]. The size of the system (92 mm × 92 mm × 105 mm), approximately is the equivalent of 1U, and has a wet mass lower than 1.20 kg and a dry mass of 0.80 kg. This means that only 0.40 kg of water are needed to produce a specific impulse of 70 s and a total impulse of 250 Ns. AQUARIUS counts a total of 5 thrusters, one for the ΔV and four as reaction control. The first one delivers a thrust of 4 mN while the others a thrust < 1 mN, with a minimum impulse bit of 0.5 mNs. The propulsion unit has been tested on ground and deployed to space from the International Space Station in 2019.

Another version of water-propelled micro-thrusters is the Free Molecular Micro-Resistojet (FMMR) developed at the Space Engineering Department at Delft University of Technology [20]. The working principle is based on sublimating ice to maintain the pressure inside the tank equal to the vapor pressure (600 Pa at 0 °C). The sublimation absorbs some heat from the ice and lowers its temperature. The same amount of heat lost is pumped by a heater into ice, to maintain the temperature and vapor pressure in the tank constant. Some ice vapor molecules move from the tank through the feed system into a plenum, kept at a pressure lower than 150 Pa, causing a decrement of tank pressure below the vapor pressure, which results in further ice sublimation, restarting the cycle. The molecules in the plenum then flow through one or more heating sections with high temperature walls, which also act as expansion slots. Tests have been performed with 50 g of propellant and changing the plenum pressure and walls temperature, between 50 Pa and 150 Pa and in the range 300-900 K respectively. The highest performances are obtained, as expected, with the upper extreme conditions, i.e. 150 Pa and 900 K. In this case, the thrust achievable is 1.4 mN, with a specific impulse of 109.9 s and a total one of 53.9 Ns.

The propulsion unit proposed by [21] considers aluminum wool as fuel and a mixture of sodium hydroxide and water as oxidizer. Hydrogen and water vapor produced by the reaction between aluminum and oxidizer are expanded through the nozzle. The assembly, shown in Figure 4.2, consists of a reaction chamber with a nozzle, a plenum volume, two oxidizer tanks with bladders, two cool gas generators and three Lee extended performance valves. The concept has been tested using 6 g of aluminum, 2 g of water and 1 g of sodium hydroxide. The results show that almost 98% of the exhaust gas is composed by water vapor and the rest of hydrogen. The energy used for the generation of thrust is only the 4% of the total energy developed by the reaction, the majority is used to evaporate water. It has been observed that, starting from a vacuum condition in the reaction chamber, pressure reaches up to 1.6 bar while temperature increases of 60 °C. The level of thrust reached is 4.7 mN, with specific and total impulse of 45 s and 0.6792 Ns, respectively.

DOI: 10.13009/EUCASS2023-801

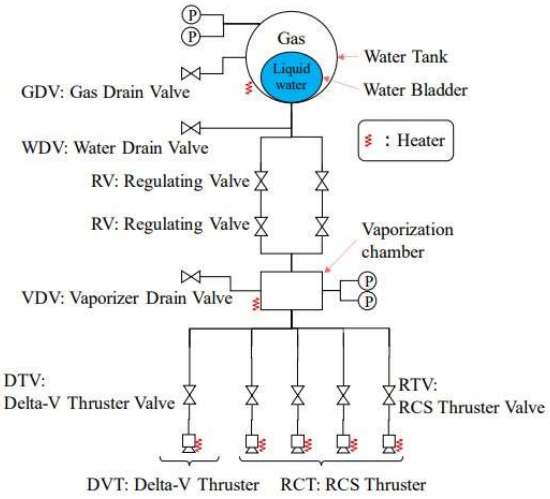

Figure 4.1: Scheme of the AQUARIUS propulsion unit [19].

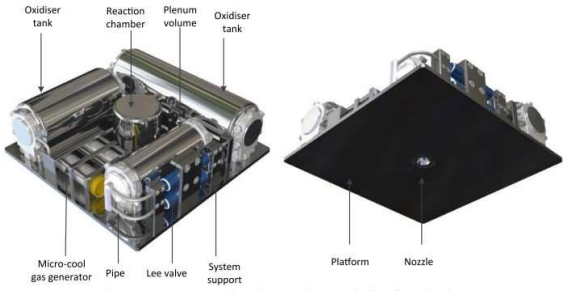

Figure 4.2: Assembly of the Al-wool-fueled system [21].

The three described technologies are briefly compared under the respective operating conditions and the main parameters are summarized in Table 4.1. In all the three systems water vapor is expanded to generate thrust. AQUARIUS and the FMMR have the same principle of a resistojet: water vapor is accelerated increasing the temperature by heaters. In the first case water is in liquid state and energy is needed for its vaporization, while in the second case ice is sublimated and vapor is obtained simply exploiting physics. Conversely, in the case of the Al-wool unit, water reacts exothermically with aluminum to produce hydrogen. The energy released by the reaction is absorbed by water, which evaporates. Thrust is mainly due to the pressure increase in the reaction chamber, given by the generation of vapor and hydrogen within it. The main advantage of this system is that no external power supply is needed. It also provides the highest thrust among the systems shown, but on the downside it has a very low total impulse. Indeed, the aluminum wool in contact with the oxidizer produces hydrogen and water vapor until the reaction is complete. When the reaction is over, the fuel needs to be replaced. The configuration presented allows only one firing, unlike the other two, which allow multiple activation. Although the aluminum wool technology is still at the beginning, it appears promising, offering benefits in terms of power and thrust.

Table 4.1: Comparison of various water micro-propulsion system.
Operating conditions referred to the temperature and pressure in the reaction chamber.
Power is the amount transferred to the propellant.

	AQUARIUS	FMMR	Al-wool
Propellant	H_2O (l)	H_2O (cr)	H_2O (l), NaOH, Al
Operating pressure [Pa]	100000	50	0
Operating temperature [K]	303	300	306
Thrust [mN]	4	0.28	4.7
Specific impulse [s]	70	63.7	45
Total impulse [Ns]	250	31.2	0.679
Wet mass [g]	1200	330	132
Propellant mass [g]	400	50	9
Power [W]	20	1.46	-

5. An innovative water propulsion system

During the experimental campaign of hydrogen production, described in Section 3, a significant increase in water temperature inside the reaction container is observed. The exothermic reaction confinement in a reduced volume allows exploiting the heat released, promoting hydrogen generation thanks to a positive feedback effect. Reducing the available water quantity up to its complete vaporization during the reaction, it is possible to increase the enthalpies of

DOI: 10.13009/EUCASS2023-801

the generated hydrogen and water vapor to obtain thrust through their expansion in a nozzle. In the majority of the currently available water micro-propulsion units, as the already mentioned AQUARIUS, water is vaporized and then steam is expanded. In these systems, the most power-consuming process is vaporization, since the water latent heat of vaporization is approximately five times the energy required to bring the same amount of water from 20 to 100 °C. In space applications, power is mainly supplied by an external power source, which is usually limited, especially in small satellites. Employing the aluminum-water reaction heat to generate steam is a possible solution to reduce the electrical power requirement. The Al-wool unit already presented exploits the reaction heat to vaporize water. The objective is to demonstrate the feasibility of a similar system in which the Al-wool is replaced by more reactive activated aluminum powder composites.

5.1 Preliminary Analysis

The suitable mass of water to be used in a propulsion unit exploiting the Al-water reaction is a key-point of the design. If the quantity is too low, the reaction may not arrive at completion, if it is too high the water does not completely vaporize. For a system conceived for space applications, it is important to avoid water in excess, as the extra weight increases launch costs. Understanding the amount of energy released by the reaction is useful to establish which reaction the reactants undergo. In the byproducts, traces of $Al(OH)_3$ and AlOOH are found, respectively the products of Eq. (1.1) and Eq. (1.2). Since it is not possible to correctly estimate the proportion of the two byproducts the less exothermic reaction (Eq. 1.1) is selected as the most conservative. The energy released in this case is $\Delta H_{r,298} = -839$ kJ/mol. The mass of water to be vaporized is estimated through calorimetry Eq. (5.1):

$$\Delta H_{r,298nAl} = (m_{H2}\, C_{H2} + m_{AlOH3}\, C_{AlOH3} + m_{H2O}\, C_{H2O})\,(T_f - T_i) + m_{H2O}\,\lambda \tag{5.1}$$

To use this equation, some assumptions must be made. The equation depends on the final and initial temperature of the mixture, assuming that all the chemical species involved have the same temperature in each instant. The mass of water in the equation refers only to the water that vaporizes. The water needed for the reaction is not included and is accounted separately. To simplify the problem, the reacting water is simply algebraically added to the mass of water coming from the equation. Only water and reaction byproducts are heated up. This is not completely correct since part of the water starts evaporating before all the aluminum powder has reacted and a small part of the energy is absorbed by it as well. The latent heat of vaporization and the specific heat capacities are constant. The values used are the ones corresponding to the pressure at the initial time. Heat losses are not accounted for in this analysis. The thermodynamic conditions considered for the calculation are pressure equal to 1 bar, initial temperature T_i at 25 °C and final temperature T_f equal to 100 °C, the boiling temperature of water at ambient pressure. The masses of hydrogen and aluminum hydroxide are found from stoichiometry starting from a defined mass of powder. For the powder used in the experiments, with composition 90% Al - 5% Bi - 5% NaCl, the theoretical amount of steam that can be produced with 1 g of powder is 10.6 g. Adding to the mass of vaporized water the 2 g of water consumed in the reaction to form the products, the total quantity of water that has to be used is 12.6 g.

5.2 CEA analysis

Analyses using NASA CEA software are performed to quantify the theoretical performances of the technology. Hydrogen is imposed as fuel and $H_2O_{(g)}$ as oxidizer in a rocket problem in equilibrium conditions to study their expansion. Their initial temperatures and pressures correspond to the boiling points of water. Equilibrium and a low expansion ratio of 14 are imposed to grant the convergence of the software. The outcome of the analysis is resumed in Table 5.1.

Table 5.1: Theoretical specific impulse from NASA CEA software, at various initial conditions, for: OF = 95 (12.6 g of H_2O(g), 0.112 g of H_2 per 1 g of Al); OF = 85 (7.5 g of H_2O (g), 0.111 g of H_2 per 1 g of Al) .

Starting Conditions		Specific Impulse [s]	
T [K]	P [bar]	OF = 95	OF = 85
373	1	117	118
393	2	120	120
406	3	121	121
414	4	107	111

The results show a specific impulse which is competitive with the current cold gas thruster technologies (in the range of 60 - 250 s), in addition to the advantages of the aluminum-water reaction in terms of volume compared to pressurized gases.

To validate a thruster that exploits the Al-water reaction, a prototype thruster and a test stand are built and pressure and thrust measurements are performed. The design is driven by the need to obtain a pressure level suitable for a thrust.

DOI: 10.13009/EUCASS2023-801

The prototype thruster in Figure 5.1a is composed of a steel reaction chamber, for the water and powder reaction, closed by two caps enclosed by four threaded rods. The lower aluminum cap is connected to the load cell. The upper cap is 3D-printed in PETG and has a nozzle, as shown in Figure 5.1b. The sizes of the thruster and the nozzle are summarized in Table 5.2. The reaction chamber size is chosen to contain the reactants and keep the powder as compact as possible in order to favor the reactivity of the process. The expansion ratio ϵ is set at 40 and it is taken from the nozzle designed by David and Knoll for their thruster [21]. For the angles of the convergent and divergent, typical α_c and α_d, literature values are used, reported in Table 5.2.

Figure 5.1a: Prototype thruster.

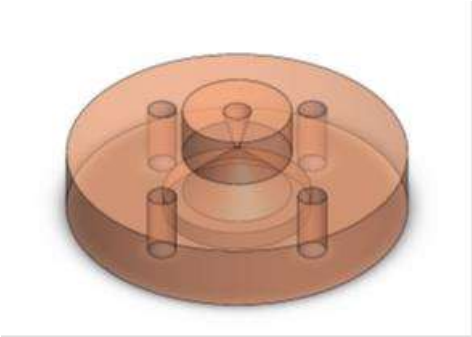

Figure 5.1b: Detail of the upper cap for the thruster. CAD model of the 3D-printed nozzle.

Table 5.2: Thruster geometrical properties.

Reaction chamber		Nozzle			
Diameter	Height	D_t	ε	a_c	a_d
mm	mm	mm	-	°	°
30	70	1	40	15	30

To guarantee that all the vapor and hydrogen produced contribute to the pressure increment, both the water and the powder must be located in the reaction chamber before the beginning of the test. The contact of water with powder, even in small quantities, must be prevented. A thermal barrier is used inside the chamber to limit heat losses. To avoid the dispersion of powder during the gas generation, a small packet, made of a stretchy synthetic fabric to contain the powder, is used. This allows the passage of water and can withstand the increase in volume from aluminum to byproducts without breaking the package.

The tests are performed using 0.7 g of powder and, as a consequence, 8.7 g of H_2O (1.2 g for the reaction and 7.5 g evaporated) for the powder 90% Al - 5% Bi - 5% NaCl and 7.5 g of water (1.1 g for the reaction and 6.4 g evaporated) for the powder 80% Al - 10% Bi - 10% NaCl. The choice to use only 0.7 g comes from preliminary tests performed without the package, showing that for the investigated system a mass of 0.7 g resulted the best compromise without the leakage of byproducts from the chamber. The sensors used for the tests are a pressure transducer, screwed on the side of the reaction chamber, and a load cell, connected to the base of the thruster and to the test stand, whose accuracy is only ± 0.1 g., acceptable for this preliminary experimental campaign.

The test stand, sketched in Figure 5.2, simply consists of a steel base at which the load cell is screwed.

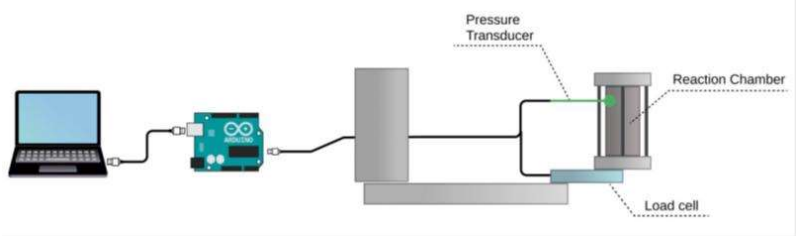

Figure 5.2: Sketch of the test stand for thrust measurements.

DOI: 10.13009/EUCASS2023-801

Pressure and thrust measurements are reported in Figure 5.3, which shows three tests performed under the same operating conditions. The first tests, performed using the powder (90% Al - 5% Bi - 5% NaCl), are the starting point, but the levels of thrust and pressure are too low. To improve these values, the gas generation must be faster, in order to build up higher pressure inside the chamber. For this reason, tests with a more reactive powder (80% Al - 10% Bi - 10% NaCl) are performed. The reactivity is strongly enhanced by higher specific surface area and by the presence of a greater amount of additives. The total heat released depends on the aluminum moles that react, and a faster hydrogen generation is more important than the hydrogen quantity produced in longer times. Compared to the previous investigated powder, a drastic improvement is observed. The reaction evolves with a much higher rate, detected from the slope of the pressure curves, directly related to the quantity of hydrogen generated. Pressure is greater, resulting in a thrust of one order of magnitude bigger. In Figure 5.3a pressure reaches and very likely overcomes 5 bar. Thrust (shown in Figure 5.3b) does not increase as pressure does, due to the reduction of the discharged mass in the unit of time. In addition, the nozzle being 3D-printed has irregularities and roughness in the material surface, which affect gas expansion.

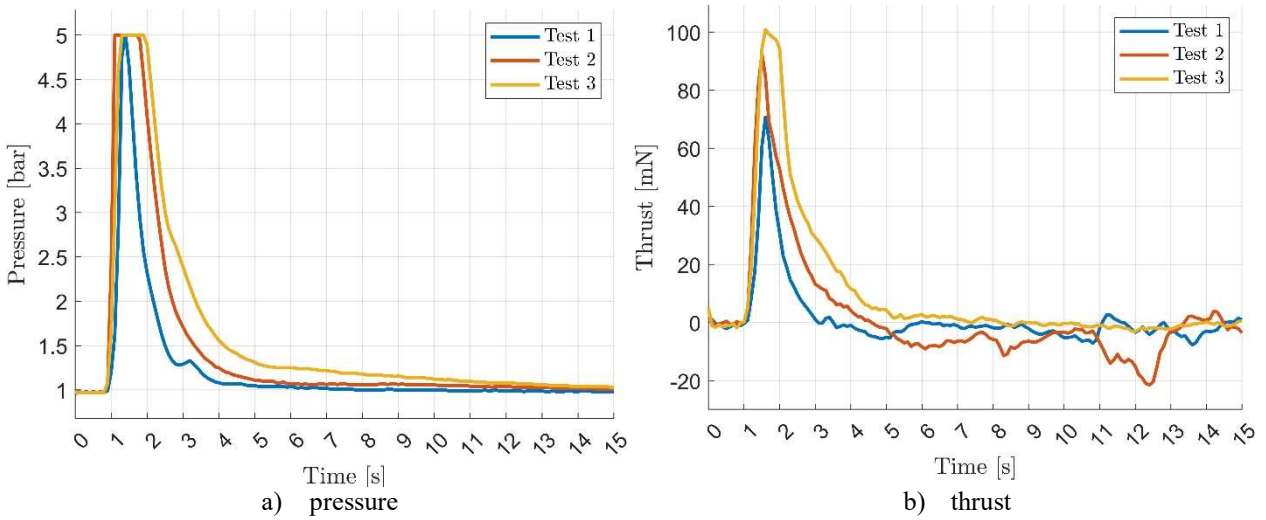

a) pressure b) thrust

Figure 5.3: Pressure and thrust measurements for powder composition 80% Al- 10% Bi - 10% NaCl.

In Figure 5.4 the time evolution of the plume shows that gases are discharged for a longer time than expected from the pressure and thrust measurements. Pressure and thrust increments are measured for a duration of approximately 3 s, while the frames reveal that a plume is clearly visible until more than 60 s from the beginning. The rate of vapor production decreases rapidly after the first few seconds and it is not sufficient to maintain high pressure.

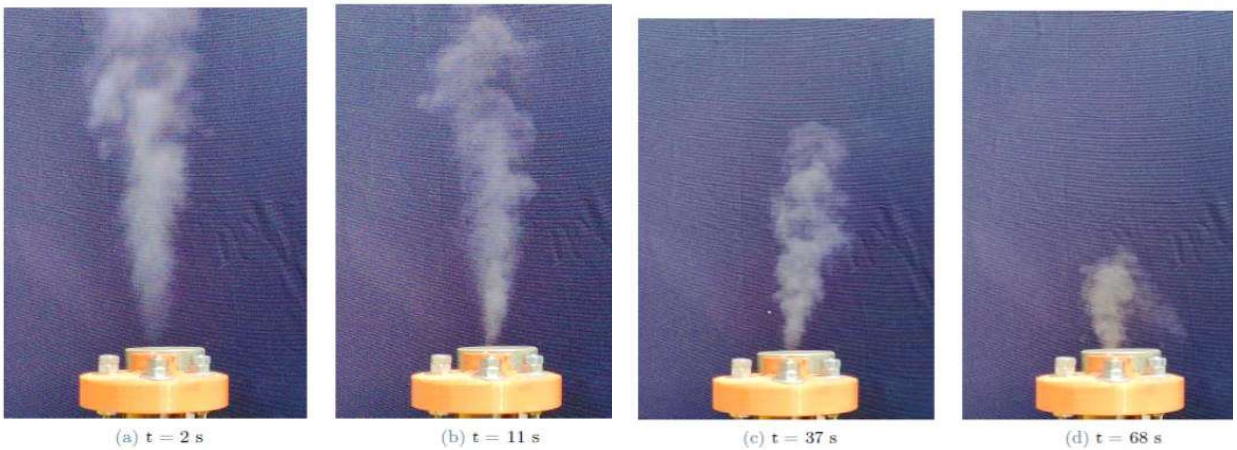

Figure 5.4: Plume evolution in time for a test with a powder composition 80% Al - 10% Bi - 10% NaCl. Time refers to seconds from the release of the powder bag in water.

DOI: 10.13009/EUCASS2023-801

The objective of this crude prototype is to exploit the more reactive aluminum composite powder in order to improve the performances of Al hydrolysis in micro-propulsion applications. Compared to Al-wool unit, this new system shows better performance and can therefore be considered interesting for further developments and future applications.

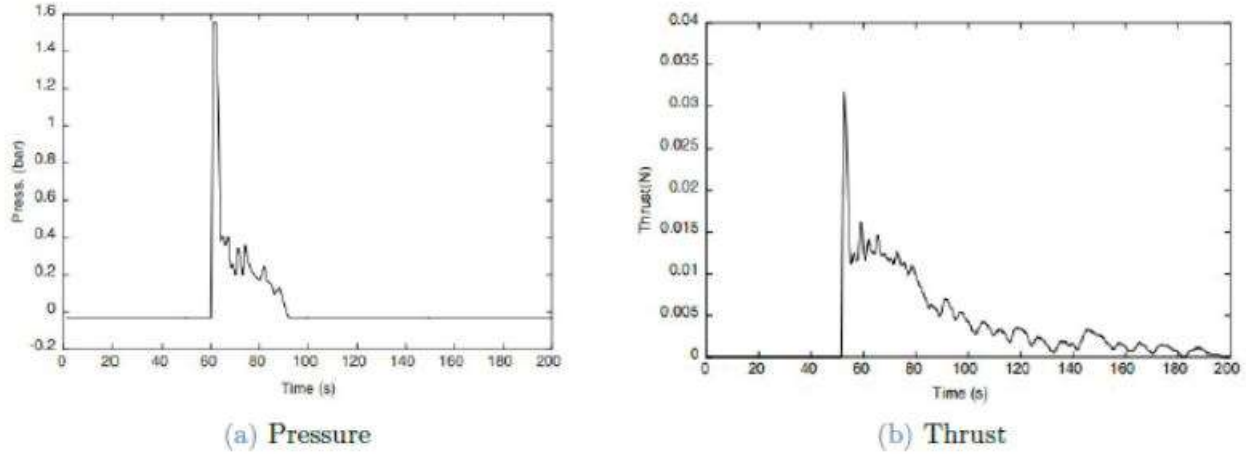

(a) Pressure (b) Thrust

Figure 5.5: Pressure and thrust behavior in the aluminum wool-fueled propulsion unit [21].

First, from Figure 5.5 pressure and thrust are comparable with the values obtained in terms of order of magnitude. However, looking at charts in Figures 5.5 it is clear that the performance is higher compared to the Al-wool engine. From Figure 5.5a, it is observed that pressure is more than doubled in almost all the investigated tests. From Figure 5.5b it is seen that thrust peaks are more than double, also considering that the values reported are underestimated. Due to the configuration of the experimental setup, the thrust acts top-down and it is measured as an increase in the engine mass by the load cell. At the same time, the vapor is discharged, resulting in a decrease in the mass of the system. Both the estimation of this contribution, in order of grams (mg), and of the thrust, is difficult to be determined with the current very simplified setup. The main difference between the tested technology ad the Al-wool unit is the duration of the firing. In the designed system, the maximum thrust duration is 10 seconds, while the Al-wool motor is capable of providing up to 100 s. Due to the poor accuracy of the load cell, small variations in the load applied may not be registered. The profile of the Al-wool unit Figure 5.5b shows a maximum peak similar to the one registered in the tests of this investigation and, after it, a series of small peaks. Figure 5.4d shows that after 68 seconds from the beginning of the reaction, gases are still exiting the engine, therefore small peaks in thrust are likely to be present but they are not detected by the load cell. David and Knoll [21] tested their system in a controlled environment in vacuum conditions, while the tests described in this chapter are performed in the open air, under variable environmental conditions. Despite the limitations of the test facility, the aluminum powder engine proves to have some substantial advantages over the aluminum-wool-fueled system. In that system, 6 g of Al-wool and 3 g of oxidizer, a basic solution made by water and NaOH, are required to expand 1.54 g of gases (98 % steam and 2 % H_2) through the nozzle [21]. In the tested configuration, instead, only 0.7 g of powder and 7.5 g of water are used to vaporize almost all the water, which means that with a lower amount of aluminum the quantity of gases that can be expanded is 5 times higher.. In addition, the measured peak thrust, despite being underestimated, proved to be at least 2 times higher than the one of the wool unit.

6. Conclusions and future developments

The paper presents the results of hydrogen production via hydrolysis of ball-milled aluminum composites and the use of this technology for the development of propulsion systems for nano- and micro-satellites with on-board hydrogen production by exploiting the reaction of aluminum in water.

Concerning the hydrogen production, it is shown that using ball-milled activated composites powders significant amounts of hydrogen can be produced. As for the specific activated powder under investigation in this study, the effects of important operating variables such as temperature and pressure of the reactant mixture are investigated. Characterisation of the original and activated powders using SEM, XRD and EDS techniques allows the significant parameters of the activation process to be identified with a view to their optimisation.

As far as the development of a water propulsion system for nano- and micro-satellites is concerned, a proof of concept device is presented. Despite the intentional essentiality and simplicity of the experimental bench developed, whose function is to verify the feasibility and implementation of a new propulsion system, the results are very promising and can lead to further investigation and development of this technology.

DOI: 10.13009/EUCASS2023-801

Future developments include an extensive experimental campaign to study new and more efficient formulations for hydrogen production, and the redesign of an experimental facility to study water propulsion systems with on-board hydrogen generation using hydrolysis of ball-milled aluminum composites.

References

[1] Yavor, Y., Goroshin, S., Bergthorson, J.M., and Frost, D.L., Comparative reactivity of industrial metal powders with water for hydrogen production, International journal of hydrogen energy, 40(2):1026–1036, 2015.

[2] Yavor, Y., Goroshin, S., Bergthorson, J.M., Frost, D.L., Stowe, R., and Ringuette, S., Enhanced hydrogen generation from aluminum–water reactions, International journal of hydrogen energy, 38(35):14992–15002, 2013.

[3] Xiao, F., Yang, R., and Liu, Z., Active aluminum composites and their hydrogen generation via hydrolysis reaction: A review, International Journal of Hydrogen Energy, 47(1):365–386, 2022.

[4] Jia, Y., Shen, J., Meng, H., Dong, Y., Chai, Y., and Wang, N., Hydrogen generation using a ball-milled Al/Ni/NaCl mixture, Journal of Alloys and Compounds, 588:259–264, 2014.

[5] Razavi-Tousi, S., and Szpunar, J., Effect of addition of water-soluble salts on the hydrogen generation of aluminum in reaction with hot water, Journal of Alloys and Compounds, 679:364–374, 2016.

[6] Liu, Z., Xiao, F., Tang, W., Cong, K., Li, J., Yang, R., and Hao, J., Study on the hydrogen generation performance and hydrolyzates of active aluminum composites, International Journal of Hydrogen Energy, 47(3):1701–1709, 2022. Merkus, D.H.G., Particle Size Measurements: Fundamentals, Practice, Quality, Springer, 2009.

[7] Godart, P., Fischman, J., Seto, K., and Hart, D., Hydrogen production from aluminum water reactions subject to varied pressures and temperatures, International Journal of Hydrogen Energy, 44(23):11448–11458, 2019.

[8] Haller, M.Y., Carbonell, D., Dudita, M., Zenhäusern, D., and Häberle, A., Seasonal energy storage in aluminium for 100 percent solar heat and electricity supply, Energy Conversion and Management: X, 5:100017, 2020.

[9] Haller, M.Y., Amstad, D., Dudita, M., Englert, A., and Häberle, A., Combined heat and power production based on renewable aluminium-water reaction, Renewable Energy, 174:879–893, 2021.

[10] Chen, C., Lan, B., Liu, K., Wang, H., Guan, X., Dong, S., and Luo, P., A novel aluminum/bismuth subcarbonate/salt composite for hydrogen generation from tap water, Journal of Alloys and Compounds, 808:151733, 2019.

[11] Bramani, N., Exploratory investigations of techniques for hydrogen generation from water hydrolysis by aluminum, Master's thesis, DAER Dept., Politecnico di Milano, 2020.

[12] Sgarzi, R., Mechanically activated Al-based powders for efficient hydrogen generation from water, Master's thesis, DAER Dept., Politecnico di Milano, 2019.

[13] Chen, C., Lan, B., Liu, K., Wang, H., Deng, Y., Zuo, Y., Xu, X., Chen, C., Chen, Z., Luo, P., et al., Preparation of Al Bi-NaCl composites and evaluation of their hydrogen production performance, Materials Research Express, 6(4):046532, 2019.

[14] Chen, C., Guan, X., Wang, H., Dong, S., and Luo, P., Hydrogen generation from splitting water with AlBi(OH)3 composite promoted by NaCl, International Journal of Hydrogen Energy, 45(24):13139–13148, 2020.

[15] Lee, J.S., Kim, H.S., Park, N.K., Lee, T.J., and Kang, M., Low temperature synthesis of α-alumina from aluminum hydroxide hydrothermally synthesized using [Al(C2O4)x (OH)y] complexes, Chemical engineering Journal, 230:351–360, 2013.

[16] Xiao, F., Yang, R., Gao, W., Hu, J., and Li, J., Effect of carbon materials and bismuth particle size on hydrogen generation using aluminum-based composites, Journal of Alloys and Compounds, 817:152800, 2020.

[17] VL53L0X Manual. STMicroelectronics, 1 edition, 5 2016.

[18] Asakawa, J., Yaginuma, K., Tsuruda, Y., Koizumi, H., Nakagawa, Y., Kakihara, K., Yanagida, K., Aoyanagi, Y., Matsumoto, T., Matsushita, S., et al., AQT-D: Demonstration of the Water Resistojet Propulsion System by the ISS-Deployed CubeSat, 33rd Annual AIAA/USU - Conference on Small Satellites, 2019.

[19] Asakawa, J., Koizumi, H., Nishii, K., Takeda, N., Murohara, M., Funase, R., and Komurasaki, K., Fundamental ground experiment of a water resistojet propulsion system: AQUARIUS installed on a 6U CubeSat: EQUULEUS, Transactions of the Japan Society for Aeronautical and Space Sciences, Aerospace Technology Japan, 16(5): 427 – 431, 2018.

DOI: 10.13009/EUCASS2023-801

[20] Cervone, A., Zandbergen, B., Guerrieri, D.C., De Athayde Costa, M., Silva, M., Krusharev, I., and Van Zeijl, H., Green micro-resistojet research at Delft University of Technology: new options for Cubesat propulsion, CEAS Space Journal, 9: 111–125, 2017.
[21] David, A.O. and Knoll, A.K., Experimental Demonstration of an Aluminum-Fueled Propulsion System for CubeSat Applications, Journal of Propulsion and Power, 33 (5):1320–1324, 2017.
[22] Petrovic, J., and Thomas, G., Reaction of aluminum with water to produce hydrogen, Technical report, U.S Department of Energy, 2008.